Published in final edited form as:

FEBS J. 2023 October ; 290(20): 4864–4876. doi:10.1111/febs.16880.

CD24 targeting with NK-CAR immunotherapy in testis, prostate, renal and (luminal-type) bladder cancer and identification of direct CD24 interaction partners

Christian Söhngen[1,*], **David J. Thomas**[1,*], **Margaretha A. Skowron**[1,*], **Felix Bremmer**[2], **Markus Eckstein**[3], **Anja Stefanski**[4], **Marc D. Driessen**[4], **Gamal A. Wakileh**[1,5], **Kai Stühler**[4], **Peter Altevogt**[6,7], **Dan Theodorescu**[8,9], **Rüdiger Klapdor**[10], **Axel Schambach**[10,11], **Daniel Nettersheim**[1,+]

[1]Department of Urology, Urological Research Laboratory, Translational UroOncology, Medical Faculty and University Hospital Düsseldorf, Heinrich Heine University Düsseldorf, Germany

[2]Institute of Pathology, University Medical Center Goettingen, Goettingen, Germany

[3]Institute of Pathology, Friedrich Alexander University Erlangen-Nürnberg, University Hospital, Erlangen, Germany

[4]Molecular Proteomics Laboratory, Heinrich-Heine-University Düsseldorf, Düsseldorf, Germany

[5]Department of Urology, University Hospital Ulm, Ulm, Germany.

[6]Skin Cancer Unit, German Cancer Research Center (DKFZ), Heidelberg, Germany.

[7]Department of Dermatology, Venereology and Allergology, University Medical Center Mannheim, Ruprecht-Karl University Heidelberg, Germany.

[8]Samuel Oschin Comprehensive Cancer Institute, Cedars-Sinai Medical Center, Los Angeles, CA, USA.

[9]Department of Surgery, Cedars-Sinai Medical Center, Los Angeles, CA, USA.

[10]Department of Gynecology and Obstetrics, Hannover Medical School, Hannover, Germany

[11]Institute for Experimental Hematology, Hannover Medical School, Hannover, Germany

[+]corresponding author: Prof. Dr. Daniel Nettersheim, Department of Urology, Urological Research Laboratory, Translational UroOncology, Medical Faculty and University Hospital Düsseldorf, Heinrich Heine University Moorenstraße 5, 40225 Düsseldorf, Germany, Daniel.Nettersheim@med.uni-duesseldorf.de, Phone: +49 211 81 06731.

[*]contributed equally

Author Contribution

conception and design: DN

acquisition of data: CS, DJT, MAS, FB, ME, ASt, GAW, MDD, DN

analysis and interpretation of data: CS, DJT, MAS, FB, ME, ASt, MDD, GAW, DN

visualization: MAS, ME, MDD, DN

drafting of the manuscript: MAS, DN

critical revision of the manuscript: FB, ME, RK, ASc

statistical analysis: CS, MAS, ME, ASt

obtaining funding: DN, FB

administrative, technical, or material support: KS, PA, DT, RK, ASc

supervision: DN

Conflict of Interest:

All authors declare that they have no conflicts of interest.

Abstract

Alternative therapeutic options targeting urologic malignancies, such as germ cell tumors, urothelial, renal and prostate carcinoma, are still urgently needed. The membrane protein CD24 represents a promising immunotherapeutical approach. This study aimed to decipher the molecular function of CD24 *in vitro* and evaluate the cytotoxic capacity of a third-generation NK cell CAR against CD24 in urologic tumor cell lines. Up to 20 urologic tumor cell lines and several non-malignant control cells were included. XTT assays and Annexin V / propidium iodide flow cytometry analyses were performed to measure cell viability and apoptosis rates, respectively. Co-immunoprecipitation followed by mass spectrometry analyses identified direct interaction partners of CD24. Luciferase reporter assays were used to functionally validate transactivation of *CD24* expression by SOX2. *N*- and *O*-glycosylation of CD24 were evaluated by enzymatic digestion and mass spectrometry. This study demonstrated that SOX2 transactivates *CD24* expression in embryonal carcinoma cells. In cells of different urological origins, CD24 interacted with proteins involved in cell adhesion, ATP binding, phosphoprotein binding, and post-translational modifications, such as histone acetylation and ubiquitination. Treatment of urological tumor cells with NK-CD24-CAR cells resulted in a decreased cell viability and apoptosis induction specifically in $CD24^+$ tumor cells. Limitations include the *in vitro* setting, which still has to be confirmed *in vivo*. In conclusion, here we identified CD24 as a promising novel target forimmune therapeutic approaches targeting urologic malignancies.

Graphical abstract text

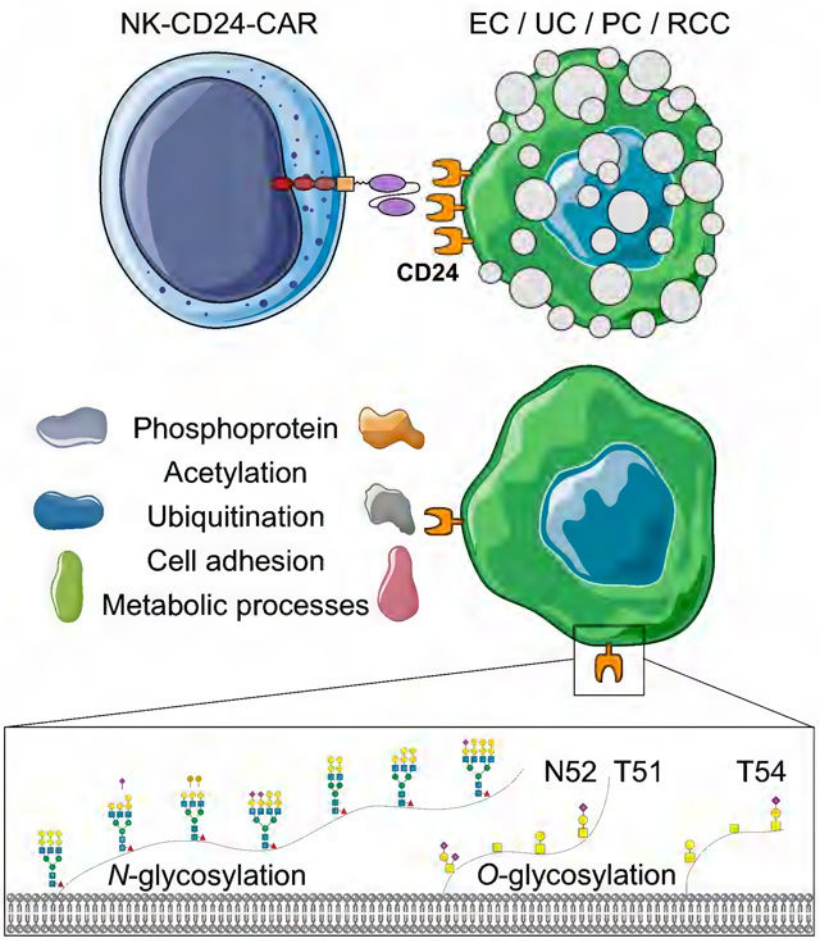

This study demonstrated the therapeutic efficacy of using NK-CD24-CAR cells for the treatment of CD24^{+} urologic malignancies *in vitro*. Immunoprecipitation followed by mass spectometry analyses identified *bona fide* interaction partners of CD24 to be involved in posttranslational modifications, cell adhesion, and metabolic processes. Moreover, the glycosylation pattern of CD24 and the SOX2-dependent regulation of expression were investigated to further enlighten its molecular function.

Keywords

CD24; immunotherapy; testicular germ cell tumor; urologic malignancies

Introduction

The signaling molecule CD24 is involved in the regulation of migration, invasion, adhesion, and metastasis [1]. *CD24* amplifications have been associated with poor prognosis in several tumor entities, such as breast, ovarian, and lung cancer [2, 3]. In a previous study, we investigated the molecular function of CD24 in germ cell tumors (GCT). We noted especially embryonal carcinoma (EC) as highly positive for CD24 in comparison to other GCT subtypes and non-malignant cells [4]. In GCT cells, we demonstrated that

CD24 expression is not only influenced by DNA methylation and histone acetylation, but also by the pluripotency factor SOX2, which is able to bind upstream of the *CD24* promotor [4]. Hence, further mechanisms of *CD24* regulation and function, as well as its therapeutic targetability by an immune therapy have yet to be deciphered [3]. Consequently, this study aimed at analyzing the SOX2-dependent regulation of *CD24* and the direct interaction partners of CD24 in EC cells. Additionally, this study evaluated the suitability of a third-generation CAR against CD24 as an immunotherapeutic option for $CD24^+$ urological malignancies, such as GCT, urothelial (UC), renal cell (RCC) and prostate carcinoma (PC).

Results

In a previous study, we evaluated the (epi)genetic and molecular regulation of *CD24* and its role in GCT biology [4]. Even though it has been shown that *CD24* expression was elevated in urologic malignancies compared to non-malignant control tissues, not much has been reported regarding the regulation of *CD24* and its direct interaction partners in a pan-urological setting.

Expression of *CD24* in urological malignancies

First, we compared the *CD24* mRNA levels in tumor and normal tissues based on the 'The Cancer Genome Atlas' (TCGA) and 'Genotype-Tissue Expression' (GTEx) datasets to validate its targetability specifically in various tumor types. As such, 20 out of the 31 evaluated cohorts showed higher CD24 levels compared to the respective normal tissues (Fig. S1 A). Then, we distinguished the *CD24* expression in the various subtypes of urological malignancies by screening the TCGA datasets (Fig. S1 B). Compared to $CD24^-$ seminoma, elevated *CD24* expression could be noted in papillary RCC (pRCC), RCC, UC, and PC to a comparable level as in EC (highly $CD24^+$) (Fig. S1 B) [4]. Since UC can be stratified into several subtypes (luminal, basal, squamous and neuroendocrine-like), we asked if *CD24* expression can be linked to a specific UC subtype [5] [6]. We screened the TCGA UC cohort and found clustering of *CD24* expression with genes indicative of the luminal-type of UC (*ADIRF*, *AOC2CD96*, *CRTAC1*, *MYCN*, *OSR1*, *PPARGC1B*, *RAP1GAP*, *S100A6*, *SPIRE2*) (Fig. S1 B, green boxes) [5] [6] [7]. Of note, no mutational events of *CD24* were found in the samples of the UC cohort (Fig. S1 B). Furthermore, we screened a cohort of 224 UC tissues for expression and membraneous localization (staining intensity from 0 to 3+) of *CD24* / CD24 by re-evaluating RNA-seq data and performing IHC (Fig. 1 A; Data S1 A) [7] [8]. Here, in UC tissues we found that an increasing membraneous staining intensity significantly correlated with increasing *CD24* expression on RNA level and that 3+ classified patients had a poorer survival probability than 0 to 2+ patients (Fig. 1 B, C). Further, *CD24* mRNA and CD24 protein levels were evaluated in cell lines from UC (RT-112, SW-1710, VM-CUB-1, UM-UC-3, T-24), PC (DU-145, PC-3, LnCap), and RCC (Caki-1, 786-O, ACHN) (Fig. 1 D, E; Fig. S1 C, D). As controls, EC cell lines (2102EP, NCCIT, NT2/D1; $CD24^+$), choriocarcinoma (CC) cell lines (JAR, JEG-3, BeWo), yolk-sac tumor (YST) cell lines (GCT-72, 1411H, NOY-1), a seminoma cell line (TCam-2; $CD24^-$) and cisplatin-resistant subclones (-R) were included (Fig. 1 D, E) [4]. In UC (RT-112, SW-1710, VM-CUB-1), three of five cell lines were $CD24^+$, in RCC (Caki-1, 786-O) and

PC (DU-145, PC-3), two of three cell lines were $CD24^+$ on protein level (Fig. 1 E; Fig. S1 C, D).

Transactivation of *CD24* expression by SOX2

Our previous study identified a canonical SOX2 binding motif (*TTTTCAGATGCAAAT*) in proximity (3248 bp upstream) of the *CD24* transcription start site in ECs [4]. Accordingly, a positive correlation ($p = 3.57 \times 10^{-33}$) between *CD24* and *SOX2* expression could be noted in non-seminomas in the TCGA GCT cohort (Fig. 1 F). To functionally confirm the transactivation of *CD24* by SOX2, luciferase reporter assays were performed. Plasmids containing either the *CD24* promotor alone (pGL4.20_CD24-Prom) or with an additional SOX2 binding motif (pGL4.20_CD24-Prom-SOX2-BM) were transfected into $CD24^+$ / $SOX2^+$ (2102EP, NCCIT, NT2/D1), $CD24^-$ / $SOX2^-$ (JAR) or $CD24^-$ / $SOX17^+$ cells (TCam-2) (Fig. 1 G) [4, 9]. Upon normalization (empty vector (pGL4.20_empty) and Renilla plasmid), an elevated luciferase activity was noticed in 2102EP and NT2/D1 ($CD24^+$ / $SOX2^+$) transfected with the pGL4.20_CD24-Prom-SOX2-BM plasmid compared to the pGL4.20_CD24-Prom plasmid (Fig. 1 H). As expected, no difference in luciferase activity was observed in JAR ($CD24^-$ / $SOX2^-$) and TCam-2 ($CD24^-$ / $SOX17^+$) cells (Fig. 1 H).

N- and *O*-Glycosylation of CD24

CD24 is a heavily glycosylated protein and our previous analyses demonstrated that glycosylation levels differed considerably between EC cell lines, prompting us to analyze the CD24 glycosylation in urological malignancies in more detail [4] [10, 11]. Enzymatic digestions of proteins isolated from 2102EP, NCCIT, NT2/D1, RT-112, PC-3 and Caki-1 cells utilizing PNGase F (cleaves *N*-glycans) and *O*-glycosidase / neuraminidase (cleaves *O*-glycans and sialic acid) revealed that, with the exception of PC-3, exclusively *N*-glycans were cleaved (Fig. 1 I). Thus, *N*-glycosylation seems to be prominent in urological malignancies, except for PC, where *N*- and *O*-glycosylation was detectable. To comprehensively characterize the *N*- and *O*-glycosylation pattern of CD24, liquid chromatography-mass spectrometry (LC-MS) analyses of a recombinant human CD24 Fc chimera expressed in mouse myeloma cells have been performed. CD24 carries two *N*-glycosylation sequons at sites N36 and N52 [12], as well as two previously reported *O*-glycosylation sites at T41 and T51 [10]. As CD24 is notoriously inaccessible to commonly used proteases like trypsin, in this study, we used a commercial recombinant chimera to test methods for detailed analysis and mapping of glycan microheterogeneity. Indeed, using either ProteinaseK or Chymotrypsin digestion of the chimera, we were able to obtain high quality intact glycopeptide spectra, giving us 11 different glycan compositions at position N52 (exemplary glycans fitting the compositions are shown in Fig.1 I). No glycans were identified for position N36. We did however identify *O*-glycosylation sites at T51, adjacent to N52 as well at T54. Here, analysis of PNgase treated chimera resolved in spectra with a high localization confidence. Additional, presumed *O*-glycan sites, without clear localization, were observed between L19 and S27 (T22/S26/S27), between S42 and P49 (S42/S44), again, in line with previous reports [10]. Identified *O*-glycan compositions, were HexNAc(1), HexNAc(1)Hex(1), HexNAc(1)Hex(1)NeuAc(1), and HexNAc(1)Hex(1)NeuAc(2) (Data S1 B).

Identification of direct interaction partners of CD24

To identify the direct interaction partners of CD24 in a pan-urological setting, co-immunoprecipitations (Co-IP) followed by LC-MS were performed (Fig. 2 A; Data S1 B - D). As controls, CRISPR/Cas9-generated *CD24*-deficient EC cell lines (Δ*CD24*) were included (Fig. 2 A; Data S1 B) [4]. A principal component analysis (PCA) demonstrated that all CD24 Co-IPs using the SWA11 antibody clearly clustered apart from the IgG_{2a} isotype controls and, in case of EC cell lines, also apart from the Δ*CD24* cells (Fig. 2 B). We found 10 proteins (RAP2A, C6orf120, STX10, TRABD, MFSD10, GDE1, ACHE, CNTFR, TMEM104, KRT31) commonly precipitated in EC cell lines (normalized against IgG_{2a} controls and Δ*CD24* cells), representing the direct interaction partners of CD24 with high reliability (Fig. 2 C; Data S1 E). According to a DAVID gene ontology analysis, these commonly precipitated factors were glycoproteins involved in GPI-anchorage (Data S1 D), while an analysis of the putative interacting factors found in at least two of the three EC cells demonstrated involvement of these phosphoproteins in post-translational modifications, such as acetylation or ubiquitination, cell adhesion, and metabolic processes (Fig. 2 D, Data S1 D) [4]. In UC, PC and RCC cell lines (abundance ratio > 10, p-value < 0.05), biological processes involved in RNA binding and regulation of mRNA decay were predicted for the 25 commonly precipitated proteins (Fig. 2 D; Fig. S2; Data S1 E). Additionally, N-glycan biosynthesis (UC), translational termination, cadherin binding, ubiquitin-dependent protein catabolic processes (PC), rRNA metabolic processes, mitochondrial translation, leukocyte mediated immunity, and glutathione metabolism (RCC) have been noted (Fig. 2 D, Fig. S2, Data S1 E). However, no CD24 interacting protein has been found to be precipitated in all four urological entities (Fig. 2 C).

Targeting CD24 by natural killer cells equipped with a chimeric antigen receptor

We already identified CD24 as a putative target for an immune therapy in $CD24^+$ EC, i. e. treatment with the CD24 antibody SWA11 resulted in an enhanced sensitization towards cisplatin, even in cisplatin-resistant sublines [4]. Hence, to validate CD24 as a target for immune therapy in GCT, UC, PC, and RCC, we evaluated the cytotoxicity of engineered NK-92 natural killer cells containing a third-generation chimeric antigen receptor (CAR) against CD24 [3]. To confirm activation of the NK-92-CD24-CAR cells in presence of CD24, we performed IFNγ ELISAs in selected $CD24^+$ cell lines (2102EP, Caki-1, PC-3) (Fig. 3 A). Elevated IFNγ concentrations have been observed upon co-culture of $CD24^+$ cells with NK-92-CD24-CAR cells compared to co-culture with NK-92 cells (Fig. 3 A). Using the 3D culture hanging drop technique, a disruption of the cellular aggregate was noted within 48 hours (h) in $CD24^+$ 2102EP, NCCIT, and NT2/D1 cells upon co-culture with the NK-92-CD24-CAR cells (ratio 1 : 3), while this was not the case upon co-culture with NK-92 cells (Fig. 3 B). This observation was further validated on protein level, where the $CD24^+$ cell population strongly diminished upon co-culture with NK-92-CD2-CAR cells (Fig. 3 C). Next, we screened the cytotoxic effect of these NK-92-CD24-CAR cells in comparison with normal NK-92 cells over 96 h by XTT assays in 20 cell lines of different urological malignancies, including cisplatin-resistant sublines (-R), Δ*CD24*-EC cells, and non-malignant fibroblasts (Fig. 3 D; Fig. S3). A high specificity of the NK-92-CD24-CAR cells to target particularly $CD24^+$ cells could be demonstrated (Fig. 3 D). Vice versa, the cell viability was only marginally reduced in Δ*CD24* cells or cells with low CD24 levels

and non-malignant fibroblasts upon co-culture with NK-92-CD24-CAR cells (Fig. 3 D). We confirmed these observations by flow cytometry apoptosis assays using CD24 and CD56 as markers to distinguish between the tumor and immune cells, respectively (Fig. 3 E; Fig. S4). We detected a strong increase in apoptosis rates only in $CD24^+$ cells (Fig. 3 E, F, Fig. S4). Similarly, PARP cleavage was specifically observed in EC cells co-cultured with NK-92-CD24-CAR cells, while this was only marginally noted upon co-culture with NK-92 cells (Fig. 3 G). Expectedly, cleaved PARP levels remained rather unchanged in Δ*CD24* cells (Fig. 3 G).

Discussion

In this study, we evaluated the targetability of CD24 by an immune therapy-based approach and deciphered its molecular function pan-urologically.

In EC, we functionally verified that SOX2 is an upstream regulator of *CD24* expression, further strengthening the involvement of CD24 in the pluripotency landscape and an undifferentiated cell fate (Fig. 4) [4].

We detected considerable differences in CD24 glycosylation among the EC cell lines as well as in UC, PC and RCC cell lines [4]. Here, we show that CD24 is predominantly *N*-glycosylated in GCT, UC and RCC cells, while in PC cells both, *N*- and *O*-glycosylation was detected. In this study, these analyses were performed on a recombinant human CD24 Fc chimera expressed from mouse myeloma cells. While a more direct immunoprecipitation of the human CD24 *in vivo* would be preferable, we believe that, due to its size and proteolysis resistance, overexpressing systems would be the best way to access this information. In our hands, direct IP from unmodified cells yielded only minute traces of glycosylated peptides, due to still-too-strong background signals from unspecified co-precipitating proteins. Despite these challenges, we show here that analyses of both *N*- and *O*-Glycans is possible from as little as 2 μg of CD24 Fc chimera using dedicated strategies with proteases. Unsurprisingly, *N*-glycan compositions reflected the non-human expression host, while identified *O*-glycans were in line with previous reports. While Li et al. described additional *O*-glycosites by utilizing a higher amount of input [10], we focused on developing a method transferable to protein amounts received from IPs. Hence, less occupied sites were less sensitively detected. In addition, the low input strategies using ProteinaseK and Chymotrypsin did in some cases yield peptides of unfavorable composition regarding fragmentation and analysis; These problems could be overcome, but would be outside the scope of this study. Nevertheless, a better understanding of the CD24 glycosylation pattern for each urologic tumor entity is still urgently needed and might enhance the clinical relevance as a therapeutic approach. Even though others have already identified specific CD24 glycosylation sites in other models [10, 13], its pattern in urologic malignancies has yet to be unraveled.

Previously, we demonstrated that in GCT cells CD24 is involved in suppressing mesodermal and endodermal differentiation via homeobox, glyco- and phosphoproteins influencing transcription, protein processing, extracellular signaling and potassium transport [4]. In parallel, ectodermal differentiation is promoted via glyco- and phosphoproteins that

influence G-coupled receptors and cytokine-mediated signaling [4]. Here, we identified the direct interaction partners of CD24 in urological malignancies. In EC, these CD24 partners could be linked to similar molecular and biological processes as deduced in our previous study, i. e. cell adhesion, phosphoprotein binding, GPI-anchorage, ATP binding, and post-translational modifications, like acetylationand ubiquitination (Fig. 4; Data S1 C, D) [4, 14]. Thus, we reliably identified the factors, which orchestrate CD24's molecular functions in EC cells (Data S1 E). Importantly, in UC, PC and RCC cell lines, comparable biological processes were predicted for the precipitated proteins, suggesting that CD24 fulfills a quite similar molecular function in these tumors. As such, we validated previous observations by Smith et al., where Ral GTPases were shown to regulate CD24 in HeLa (cervical carcinoma) and UM-UC-3 (UC) cells [15] and Wang et al., who observed NPM1 in CD24-immunoprecipitated DU-145 (PC) cells [16]. Nevertheless, in each urological malignancy, CD24 seems to interact with a different set of proteins to mediate its molecular function (Fig. S2; Data S1 D).

Finally, we made use of NK cell-based CAR therapy to target specifically CD24. Consisting of an anti-CD24 scFv being fused to the CD28, 4–1BB, and CD3ζ domain, these NK-CD24-CAR cells become activated through secretion of IFNγ upon co-incubation with $CD24^+$ (patient-derived) ovarian cancer cells, eventually resulting in enhanced cytotoxicity in the tumor cells [3]. Here, we convincingly demonstrated that $CD24^+$ (cisplatin-resistant) cells can be targeted highly specific by NK-CD24-CAR cells, while $CD24^-$ or Δ*CD24* EC cells did not respond. In GCT, this treatment aims at $CD24^+$ EC, which represent the aggressive stem cell-like population of the non-seminomas with profound abilities to develop into chemotherapy-resistant teratomas or aggressive YST. Thus, early targeting of EC is an important step is preventing tumor progression. Regarding PC and RCC cells, although the majority of tumor tissues and cell lines was $CD24^+$, also $CD24^-$ samples were observed, arguing for an early screen for $CD24^+$ during oncological care to filter out patients that might benefit from a CD24 immune therapy. Concerning UC, here $CD24^+$ was linked to the luminal-type and CD24 membranous staining intensity correlated to a poor survival probability, suggesting that especially those $CD24^+$ patients might benefit from a NK-CD24-CAR therapy. We suggest to include screening for CD24 in routine diagnostics of UC patients to identify the patients for immunotherapy and predict overall survival probability.

This study confirmed the transactivation of *CD24* by SOX2 and demonstrated the involvement of CD24 in influencing cellular signaling and differentiation via interacting with glyco- and phosphoproteins regulating post-translational modifications. Testing CD24-targeting immune therapies seems a very promising approach in treating (cisplatin-resistant) urological malignancies, which should be translated into clinical trials in the near future.

Materials and Methods

Ethics statement

The ethics committee (EC) of the Medical Faculty of the Heinrich Heine University Düsseldorf raised no concerns on utilizing cell lines for *in vitro* experiments (vote 2018–178 to D. N.). Ethical approval for using the UC tissues in the present study was obtained from the EC of the FAU Erlangen-Nürnberg (votes 329_16B, 97_18Bc).

Cell culture

Table S1 indicates the culture conditions of the used tumor and non-cancerous cells, which are checked for short tandem repeats and mycoplasma contamination regularly. Establishment of *CD24*-deficient EC cell lines (Δ*CD24*) via CRISPR/Cas9 technology has been performed as published previously [4, 17, 18]. For three-dimensional cultivation in hanging drops, similar to our previous studies [19, 20], 3×10^3 tumor cells per drop (40 microliter (µl)) were seeded onto an inverted lid of a 15 centimeter (cm) cell culture dish before being inverted back onto the bottom chamber filled with phosphate buffered saline (PBS) for humidity. The next day, NK-92 or NK-92-CD24-CAR cells were added in the same manner at a ratio of 1 : 3 in a volume of 10 µl per drop supplemented with recombinant human IL-2 (Peprotech via Biozol, Eching, Germany, final concentration per drop 5 nanograms / milliliter (ng / ml). Visualization of cellular aggregates by microscopy was performed after 48 h.

Cell viability assay

XTT viability assays were performed as described previously [4]. For co-treatment of tumor cells (3×10^3 cells / 96-well) with NK-92 and NK-92-CD24-CAR cells, cell viability was evaluated upon addition of immune cells in various ratios (1:1, 1:3, 1:5, 1:10) 24 h after seeding of the tumor cells. Immune cells were re-applied after 48 h and viability of tumor cells was measured over 96 h in quadruplicates after replacing medium to remove immune cells.

Determination of IFNγ concentration

For the determination of IFNγ concentration, 1×10^5 tumor cells were seeded into 6-well plates and incubated for 24 h before being co-cultured with immune cells (ratio 1 : 5). Supernatants were evaluated using the human 'IFNγ Standard ABTS ELISA Development Kit' (Peprotech via Biozol, Eching, Germany) according to the manufacturer's protocol.

Flow cytometry

The CD24 protein level in pan-urologic tumor cells was evaluated by an antibody staining followed by flow cytometry as described previously [4]. To evaluate the apoptosis induction in tumor cells upon incubation with NK-92 / NK-92-CD24-CAR cells [3] (ratio tumor cells : NK-92 cells; 1 : 5), Annexin V / DAPI staining with subsequent flow cytometry has been performed similarly to previously described protocols [17]. Additionally, to distinguish between tumor and NK cell populations, samples were stained with anti-CD24-PE (1:50) and anti-CD56-APC (1:50) (both Miltenyi Biotech, Bergisch Gladbach, Germany). Before measurement, cells were washed once with 1 x Annexin V-binding buffer and kept on ice. At least 5×10^4 $CD24^+$ cells were counted and analyzed using the FlowLogic Software v7 (Miltenyi Biotech, Bergisch Gladbach, Germany). See table S2 for detailed information on the utilized antibodies (Table S2).

RNA extraction and quantitative RT-PCR

As described previously, RNA was extracted using the 'RNeasy Mini Kit' (Qiagen, Hilden, Germany) according to the manufacturer's protocol followed by *in vitro* transcription of

1 microgram (μg) using 'RNA Oligo(dT)18 Primer', dNTPs, 'RiboLock RNAse inhibitor' and 'Maxima H Minus Reverse Transcriptase' (all Thermo Fisher Scientific, Schwerte, Germany) [21]. Gene expression of *CD24* was determined in triplicates using SYBR-green-based 'Luna Universal qPCR Master Mix' (New England Biolabs, Frankfurt am Main, Germany) and 7.34 ng cDNA per sample on the CFX384 cycler (BioRad, Feldkirchen, Germany). *CD24* levels were normalized to expression of housekeeping genes *GAPDH* and *ACTB*. See table S3 for oligonucleotide sequences (Table S3).

Co-immunoprecipitation

Co-IPs were performed by using 'Dynabeads M-270 Epoxy Beads' (Thermo Fisher Scientific, Schwerte, Germany) according to the manufacturer's protocol. Briefly, 3 milligram (mg) beads coupled to 6 μg SWA11 antibody or IgG_{2a} isotype control (Santa Cruz Biotechnology, Heidelberg, Germany) and 1 mg of total protein (n = 3) were used (Table S2). LC-MS to identify interaction partners has been performed as described previously [4]. Data have been deposited to the 'ProteomeXchange Consortium' via the 'PRIDE' partner repository (PXD039063) [22].

Analysis of *N*- and *O*-glycosylation

To evaluate *N*- and *O*-glycosylation, 20 μg protein were enzymatically digested with PNGase F (500 units (U) / 1 μl), *O*-Glycosidase (40,000 U / 1 μl) and / or α2–3,6,8 Neuraminidase (100 U / 2 μl) (New England Biolabs, Frankfurt am Main, Germany) for 1 h according to the manufacturer's protocol to remove *N*-linked glycoproteins, core 1 and core 3 *O*-glycans, and terminal sialic acid residues, respectively.

Glycoproteomics of recombinant CD24 chimera

For each digestion, 2 μg of recombinant human CD24 Fc Chimera protein (5247-CD-050, R&D systems via Bio-Techne, Wiesbaden, Germany) expressed in mouse myeloma cells were brought to 50 mM triethylammonium bicarbonate (TEAB) (in total 20 μl). ProteinaseK or Chymotrypsin (both Promega, Walldorf, Germany) were added at a ratio of approximately 1 : 200 and 1 : 50 parts protein (weight / weight), respectively. Digestion was allowed to continue for 6 h at 37°C under constant shaking. Afterwards both samples were heated to 96°C for 5 minutes (min), then acidified with 0.2 % trifluoroacetic acid (TFA) in water and dried. Samples were resuspended in 0.2 % TFA and 2 % acetonitrile before being analyzed by LC-MS.

For *O*-glycan mapping, 6 μg of protein were treated with PNgase F (New England Biolabs, Frankfurt am Main, Germany) according to the supplier protocol (denaturing conditions). After *N*-glycan removal, the sample was digested with ProteinaseK, as described above and purified using C18 SPE columns before LC-MS analysis. Data was collected using either stHCD(10–34-58) fragmentation methods (*N*-glycosylation) or HCD(15)-pd-EThcD35 and stHCD(10–30-40)-pD-EThcD methods for *O*-glycans, as described before [23]. Data processing and analysis was performed using Byonic V5.0.3 (Protein Metrics). Settings were as follows: non-specific digest, variable modifications: Acetyl@Nterm; oxidation@M; PhetoAsn@F; phospho@STY, one rare and common each allowed. Glycan databases were either 309 mammalian for N-glycans or 9 common *O*-glycans (both Byonic internal).

PNgaseF treated samples were also searched against N-glycan database to ensure complete removal. Byonic results were filtered, as well as spectra visually inspected to ensure only high quality IDs. (Byonic filters: PEP 2D<= 0.1; score>= 200). Graphical illustration of potential glycans was drawn using DrawGlycan-SNFG (http://www.virtualglycome.org/DrawGlycan/) [24].

Western blot analysis

For western blot analyses, cells were lysed using RIPA buffer (Cell Signaling, Frankfurt am Main, Germany) and the protein concentrations were measured by the 'Pierce BCA Protein Assay-Kit' according to the manufacturer's protocol. 20 µg of whole protein lysates were separated by SDS-PAGE and transferred onto a polyvinylidene difluoride (PVDF) membrane (Merck Healthcare KGaA, Darmstadt, Germany) using the 'Trans-Blot Turbo' system (BioRad, Feldkirchen, Germany). After blocking, primary antibodies were incubated overnight at 4 °C followed by an 2 h incubation with secondary horseradish peroxidase-coupled antibodies at room temperature. Detection was performed using the 'ChemiDoc Imaging System' (BioRad, Feldkirchen, Germany). See table S2 for detailed information on the utilized antibodies (Table S2).

Luciferase assays

The pGL4.20_CD24–1896 (pGL4.20_CD24-Prom) plasmid has been kindly provided by Prof. Dan Theodorescu (Department of Surgery (Urology), Cedars-Sinai Medical Center, Los Angeles, USA) [25, 26]. A 374 base-pair long fragment containing the SOX2 binding motif (BM) (Genewiz / Azenta, Leipzig, Germany) has been cloned into the pGL4.20_CD24–1896 plasmid (pGL4.20_CD24-Prom) [9] using a *NheI* and *SfiI* double digestion (both New England Biolabs). The purified fragment ('Monarch DNA Gel Extraction Kit', New England Biolabs) was further ligated into a plasmid, used to transform *E.coli*, isolated from bacteria and sequenced as described previously to generate the pGL4.20_CD24-Prom-SOX2-BM construct [4]. Briefly, transformation of *E.coli* and plasmid extraction were performed using the 'TA Cloning Kit with pCR2.1 vector and One Shot TOP10 chemically competent *E. coli'* (Thermo Fisher Scientific, Schwerte, Germany) and the 'Plasmid Maxi Kit' (Qiagen, Hilden, Germany) according to the manufacturer's protocols. For verification, pGL4.20_CD24-Prom and pGL4.20_CD24-Prom-SOX2-BM plasmids were Sanger sequenced using 'CD24promSF1' and 'CD24promSR1' primer, while 'RV Primer 3' and 'M13 reverse' primers were used to verify the control plasmids pGL4.51[*luc2*/CMV/Neo] and pGL4.20[*luc2*/Puro] (pGL4.20) (both Promega, Walldorf, Germany). See table S3 for detailed information on the utilized sequencing primer (Table S3).

For the luciferase assay, transfection of 0.5 µg pGL4.20 (Promega, Walldorf, Germany), pGL4.20_CD24-Prom or pGL4.20_CD24-Prom_SOX2-BM was performed using 'FuGENE HD' transfection reagent (Promega) in a 1 : 5 (µg DNA : µl transfection reagent) ratio. Luciferase activity was determined using 'Dual Luciferase Reporter Assays' (Promega) according to the manufacturer's protocol (n = 4) and analyzed via the Perkin Elmer Wallac 1420 Victor2 Microplate Reader (Hölzel Diagnostika, Cologne, Germany). For

normalization, tumor cells were co-transfected with 0.5 μg Renilla SV40 promoter reporter plasmid (pRL-SV40P, Addgene, Teddington, United Kingdom).

Online analyses tools

'The Cancer Genome Atlas' (TCGA) and 'Genotype-Tissue Expression' (GTEx) datasets were analyzed using the 'cBioPortal' (https://www.cbioportal.org/) or 'GEPIA' (http://gepia.cancer-pku.cn/) online tools [27–29]. For interaction prediction, the STRING algorithm was used (https://string-db.org) [30]. Molecular functions of LC-MS data were predicted using the 'DAVID Functional Annotation Tool' based on 'GOTERM_BP_DIRECT, 'GOTERM_MF_DIRECT', 'INTERPRO', 'UP_KW_MOLECULAR_FUNCTION', 'UP_KW_BIOLOGICAL_PROCESS', 'UP_KW_PTM' and 'KEGG_PATHWAY' (https://david.ncifcrf.gov) [31]. LC-MS data were visualized by 'Venny' (https://bioinfogp.cnb.csic.es/tools/venny/) [32], 'imageGP' (http://www.bic.ac.cn//) [33], and PCA ('PCAGO', https://pcago.bioinf.uni-jena.de) [34].

Supplementary Material

Refer to Web version on PubMed Central for supplementary material.

Acknowledgements

We kindly thank Anna Pehlke for excellent technical assistance.

We kindly thank PD Dr. Michèle Hoffmann, Dr. Christoph Oing, Prof. Dr. Michal Mego, Dr. Isabella Syring-Schmandke, Dr. Jørgen Fogh, Prof. Dr. Bernd Schmitz-Dräger, Prof. Dr. Margaret A. Knowles, Dr Janet Shipley, and PD Dr. Michael Peitz for providing cell lines and healthy control cells (see Table S1 for affiliations and provided cell lines).

D. Nettersheim was supported by the 'Deutsche Forschungsgemeinschaft' (NE 1861/8–1).

C. Söhngen was supported by the ‚Studienstiftung des Deutschen Volkes'.

F. Bremmer was supported by the 'Wilhelm Sander-Stiftung' (2016.041.1 / .2).

G. A. Wakileh supported this study during his 'Ferdinand Eisenberger' research scholarship funded by the 'Deutsche Gesellschaft für Urologie' (DGU).

D. Theodorescu was supported by the 'National Institute of Health' (NIH/NCI R01-CA75115).

Data Availability statement

LC-MS raw data generated in this study can be accessed via ProteomeXchange (http://www.proteomexchange.org) (PXD039063).

Abbreviations:

3D	Three-dimensional
ABTS	2,2'-azino-bis(3-ethylbenzothiazoline-6-sulfonic acid
APC	Allophycocyanin

bp	Base pairs
CAR	Chimeric antigen receptors
CC	Choriocarcinoma
CD24	Cluster of differentiation 24
cm	Centimeter
Co-IP	Co-immunoprecipitation
Δ*CD24*	*CD24*-deficient cell line
DAPI	4′,6-diamidino-2-phenylindole
EC	Embryonal carcinoma
ELISA	Enzyme-linked immunosorbent assay
FITC	Fluorescein isothiocyanate
GCT	Germ cell tumor
GTEx	Genotype-Tissue Expression
IHC	Immunohistochemistry
h	Hour
LC-MS	Liquid chromatography-mass spectrometry
µg	Microgram
µl	Microliter
µM	Micromolar
ml	Milliliter
min	Minute
mM	Millimolar
ng	Nanogram
NK cell	Natural killer cell
PBS	Phosphate buffered saline
PC	Prostate cancer
PCA	Principal component analysis
PE	Phycoerythrin
pRCC	Papillary renal cell carcinoma

PVDF	Polyvinylidene difluoride
-R	Cisplatin-resistant subclones
RCC	Renal cell carcinoma
SD	Standard deviation
SE	Seminoma
TEAB	Triethylammonium bicarbonate
TFA	Trifluoroacetic acid
TCGA	The Cancer Genome Atlas
UC	Urothelial carcinoma
YST	Yolk-sac tumor
XTT	2,3-bis-(2-methoxy-4-nitro-5-sulfophenyl)-2H-tetrazolium-5-carboxanilide

References

1. Altevogt P, Sammar M, Hüser L, Kristiansen G (2020) Novel insights into the function of CD24: A driving force in cancer. Int. J. Cancer
2. Wu J, Zhang L, Li H, et al. (2019) Nrf2 induced cisplatin resistance in ovarian cancer by promoting CD99 expression. Biochem Biophys Res Commun 518, 698–705 [PubMed: 31472965]
3. Klapdor R, Wang S, Morgan M, et al. (2019) Characterization of a novel third-generation anti-CD24-CAR against ovarian cancer. Int J Mol Sci. 10.3390/ijms20030660
4. Skowron MA, Becker TK, Kurz L, et al. (2021) The signal transducer CD24 suppresses the germ cell program and promotes an ectodermal rather than mesodermal cell fate in embryonal carcinomas. Mol Oncol. 10.1002/1878-0261.13066
5. Robertson AG, Kim J, Al-Ahmadie H, et al. (2018) Comprehensive Molecular Characterization of Muscle-Invasive Bladder Cancer. Cell. 10.1016/j.cell.2018.07.036
6. Nakauma-González JA, Rijnders M, van Riet J, et al. (2022) Comprehensive Molecular Characterization Reveals Genomic and Transcriptomic Subtypes of Metastatic Urothelial Carcinoma. Eur Urol. 10.1016/j.eururo.2022.01.026
7. Weyerer V, Stoehr R, Bertz S, et al. (2021) Prognostic impact of molecular muscle-invasive bladder cancer subtyping approaches and correlations with variant histology in a population-based mono-institutional cystectomy cohort. World J Urol. 10.1007/s00345-021-03788-1
8. Pfannstiel C, Strissel PL, Chiappinelli KB, et al. (2019) The tumor immune microenvironment drives a prognostic relevance that correlates with bladder cancer subtypes. Cancer Immunol Res. 10.1158/2326-6066.CIR-18-0758
9. Overdevest JB, Thomas S, Kristiansen G, et al. (2011) CD24 offers a therapeutic target for control of bladder cancer metastasis based on a requirement for lung colonization. Cancer Res 71, 3802–3811 [PubMed: 21482678]
10. Li X, Wilmanowski R, Gao X, et al. (2022) Precise O-Glycosylation Site Localization of CD24Fc by LC-MS Workflows. Anal Chem. 10.1021/ACS.ANALCHEM.2C01137/SUPPL_FILE/AC2C01137_SI_001.PDF
11. Kristiansen G, MacHado E, Bretz N, et al. (2010) Molecular and clinical dissection of CD24 antibody specificity by a comprehensive comparative analysis. Lab Investig. 10.1038/labinvest.2010.70

12. Chantziou A, Theodorakis K, Polioudaki H, et al. (2021) Glycosylation Modulates Plasma Membrane Trafficking of CD24 in Breast Cancer Cells. Int J Mol Sci 22, 8165 [PubMed: 34360932]
13. Ohl C, Albach C, Altevogt P, Schmitz B (2003) N-glycosylation patterns of HSA/CD24 from differnet cell lines and brain homogenates: A comparison. Biochimie 85, 565–573 [PubMed: 12829373]
14. Kristiansen G, Sammar M, Altevogt P (2004) Tumour biological aspects of CD24, a mucin-like adhesion molecule. J Mol Histol 35, 255–262 [PubMed: 15339045]
15. Smith SC, Oxford G, Wu Z, et al. (2006) The Metastasis-Associated Gene CD24 Is Regulated by Ral GTPase and Is a Mediator of Cell Proliferation and Survival in Human Cancer. Cancer Res 66, 1917–1922 [PubMed: 16488989]
16. Wang L, Liu R, Ye P, et al. (2015) Intracellular CD24 disrupts the ARF-NPM interaction and enables mutational and viral oncogene-mediated p53 inactivation. Nat Commun 6,
17. Müller MR, Burmeister A, Skowron MA, et al. (2022) Therapeutical interference with the epigenetic landscape of germ cell tumors: a comparative drug study and new mechanistical insights. Clin Epigenetics 2022 141 14, 5
18. Burmeister A, Stephan A, Alves Avelar LA, et al. (2022) Establishment and evaluation of a dual HDAC / BET inhibitor as a therapeutic option for germ cell tumors and other urological malignancies. Mol Cancer Ther 21, 1674–1688 [PubMed: 35999659]
19. Skowron MA, Watolla MM, Nettersheim D (2021) Three-Dimensional Cultivation of Germ Cell Cancer Cell Lines as Hanging Drops. Methods Mol Biol 2195, 77–83 [PubMed: 32852758]
20. Skowron MA, Eul K, Stephan A, et al. (2022) Profiling the 3D interaction between germ cell tumors and microenvironmental cells at the transcriptome and secretome level. Mol Oncol 1–21
21. Skowron MA, Vermeulen M, Winkelhausen A, et al. (2020) CDK4/6 inhibition presents as a therapeutic option for paediatric and adult germ cell tumours and induces cell cycle arrest and apoptosis via canonical and non-canonical mechanisms. Br J Cancer. 10.1038/s41416-020-0891-x
22. Perez-Riverol Y, Csordas A, Bai J, et al. (2019) The PRIDE database and related tools and resources in 2019: Improving support for quantification data. Nucleic Acids Res. 10.1093/nar/gky1106
23. Riley NM, Malaker SA, Driessen MD, Bertozzi CR (2020) Optimal Dissociation Methods Differ for N- and O-Glycopeptides. J Proteome Res 19, 3286–3301 [PubMed: 32500713]
24. Cheng K, Zhou Y, Neelamegham S (2017) DrawGlycan-SNFG: A robust tool to render glycans and glycopeptides with fragmentation information. Glycobiology. 10.1093/glycob/cww115
25. Thomas S, Harding MA, Smith SC, et al. (2012) CD24 is an effector of HIF-1-driven primary tumor growth and metastasis. Cancer Res 72, 5600–5612 [PubMed: 22926560]
26. Overdevest JB, Knubel KH, Duex JE, et al. (2012) CD24 expression is important in male urothelial tumorigenesis and metastasis in mice and is androgen regulated. Proc Natl Acad Sci U S A 109,
27. Gao J, Aksoy BA, Dogrusoz U, et al. (2013) Integrative analysis of complex cancer genomics and clinical profiles using the cBioPortal. Sci Signal. 10.1126/scisignal.2004088
28. Cerami E, Gao J, Dogrusoz U, et al. (2012) The cBio Cancer Genomics Portal: An open platform for exploring multidimensional cancer genomics data. Cancer Discov 2, 401–404 [PubMed: 22588877]
29. Tang Z, Li C, Kang B, et al. (2017) GEPIA: a web server for cancer and normal gene expression profiling and interactive analyses. Nucleic Acids Res 45, W98–W102 [PubMed: 28407145]
30. Szklarczyk D, Gable AL, Lyon D, et al. (2019) STRING v11: protein–protein association networks with increased coverage, supporting functional discovery in genome-wide experimental datasets. Nucleic Acids Res 47, D607–D613 [PubMed: 30476243]
31. Dennis G, Sherman BT, Hosack DA, et al. (2003) DAVID: Database for Annotation, Visualization, and Integrated Discovery. Genome Biol. 10.1186/gb-2003-4-9-r60
32. Oliveros JC Venny. An interactive tool for comparing lists with Venn's diagrams. In: Accessed 08 Jan 2022
33. Chen T, Liu Y-X, Huang | Luqi, Huang L (2022) ImageGP: An easy-to-use data visualization web server for scientific researchers. iMeta 1, e5

34. Gerst R, Hölzer M (2019) PCAGO: An interactive tool to analyze RNA-Seq data with principal component analysis. bioRxiv 433078

35. Guo CC, Bondaruk J, Yao H, et al. (2020) Assessment of Luminal and Basal Phenotypes in Bladder Cancer. Sci Reports 2020 101 10, 1–14

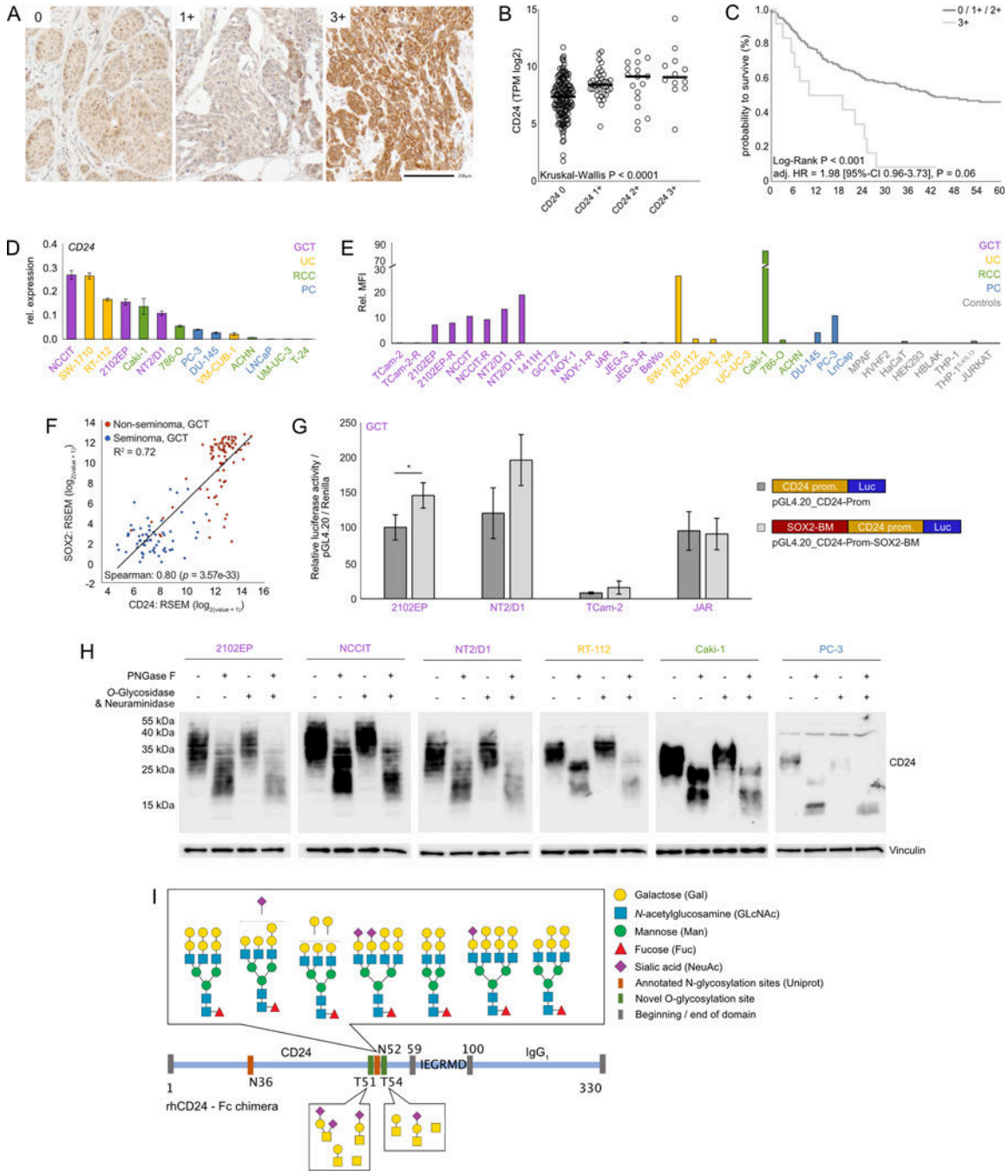

Figure 1:

A) Exemplary pictures of CD24 IHC staining in a UC cohort (n = 227). Scale bar = 200 μm B) Correlation of membranous CD24 grading (0: no membranous CD24, 1+: membranous CD24 mostly absent, only scattered cells $CD24^+$ on membrane, 2+: membranous $CD24^+$, 3+: strong membranous $CD24^+$) to *CD24* mRNA expression (as transcripts per million (TPM) in $\log_2$ scale) (n = 227). The null hypothesis that there is no difference between the analyzed groups could be rejected by Kruskal-Wallis test ($p < 0.0001$). C) Probability to survive (%) in dependence to the intensity of membranous CD24. The hazard ratio (HR) has

been adjusted for pT-stage, pN-stage, *CD24* mRNA expression, resection margin, sex, age, L, V and Pn (Data S1 A). The null hypothesis that analyzed groups have identical hazard functions could be rejected by Log-Rank test ($p < 0.001$). D) *CD24* expression in GCT, UC, RCC, and PC cell lines as evaluated by qRT-PCR (n = 3). *GAPDH* and *ACTB* served as housekeeping genes. Error bars are indicated by means of SD. E) CD24 protein levels in GCT, UC, RCC, and PC cell lines as measured by antibody staining with subsequent flow cytometry indicated as relative mean fluorescence intensities (MFI) normalized to the unstained control. Previously published data on CD24 protein levels in GCT cells have been included in the context of this study [4]. F) Correlation of *CD24* to *SOX2* expression in GCT patient samples from the TCGA cohort. G) Relative luciferase activity upon transfection with the plasmid containing the CD24 promotor (dark grey) or the CD24 promotor plus a SOX2 binding motif (light grey) (n = 4). Statistically significant differences were asterisked (Two-tailed Student's t tests, * $p < 0.05$). The relative light unit (RLU) was normalized against the empty vector and the Renilla control. Error bars are indicated by means of SD. H) Western blot analyses of CD24 in PNGase F and / or *O*-Gycosidase and Neuraminidase digested protein lysates from 2102EP, NCCIT, NT2/D1, RT-112, Caki-1, and PC-3. Vinculin served as a loading control. I) Representative CD24 glycan structures based on identified compositions. Other isomers are possible and can be derived from Data S1 B. Identification evidence from Byonic search. All glycan compositions are based on rigorously filtered results (Byonic score > 200, Pep2D < 0.1), combined from analysis of ProteinaseK or Chymotrypsin digested proteins. Created using DrawGlycan-SNFG online.

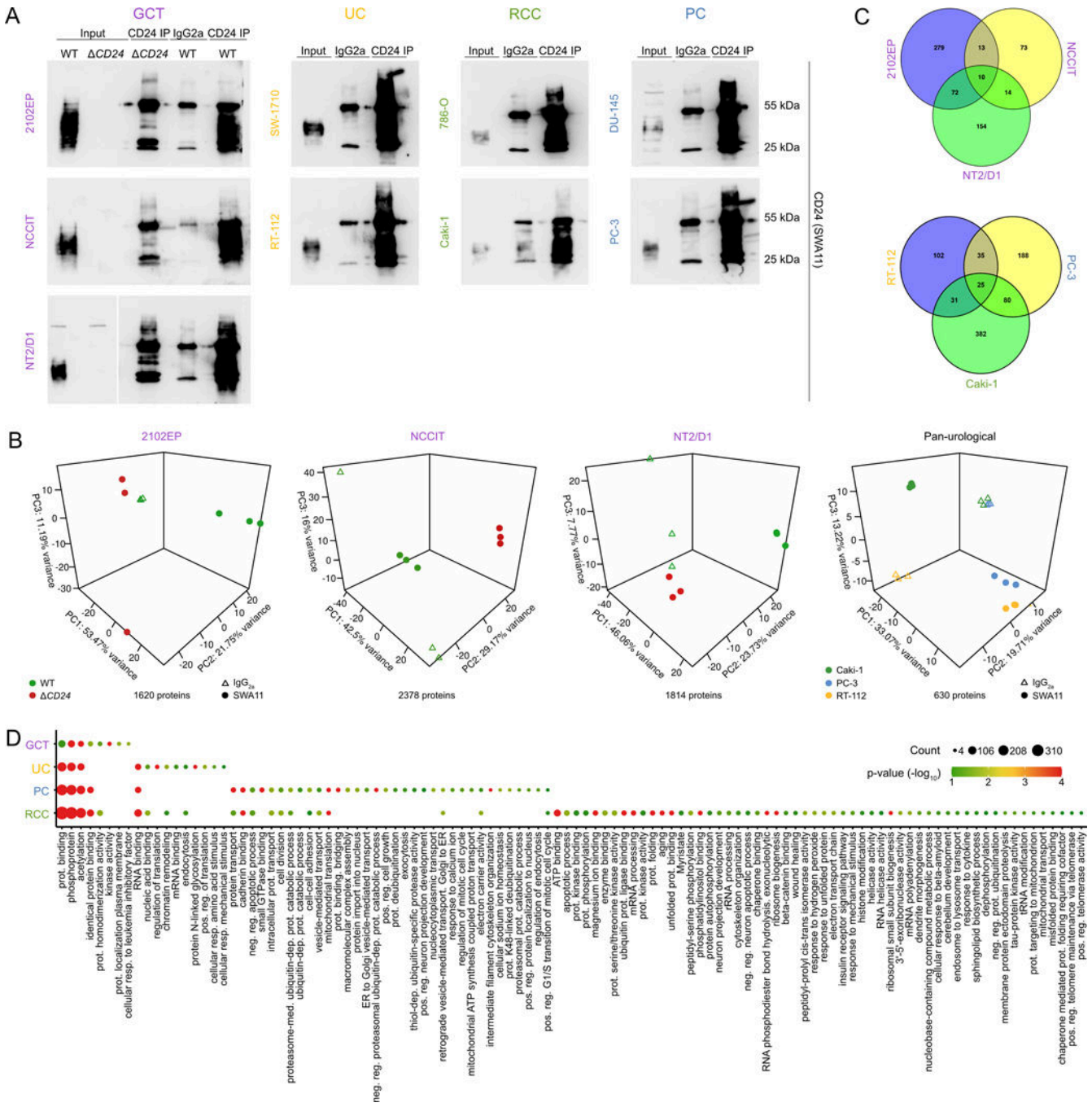

Figure 2:

A) Western blot analyses detecting CD24 in protein lysates from EC (incl. Δ*CD24* sublines), UC, RCC, and PC after co-immunoprecipitation with either a CD24 antibody (SWA11) or an IgG_{2a} isotype control in comparison to the input control (2 %, 20 μg). B) PCA plots of LC-MS data after co-immunoprecipitation with either a CD24 antibody (SWA11) or an IgG_{2a} isotype control in EC (2102EP, NCCIT, NT2/D1; including Δ*CD24* sublines), UC (RT-112), RCC (Caki-1), and PC (PC-3) (n = 3). C) Venn diagram indicating commonly interacting proteins in EC cells after normalization to the IgG_{2a} control and Δ*CD24* EC

protein lysates as well as commonly interacting proteins found in RT-112, PC-3, and Caki-1 cells. D) Enrichment plot summarizing the gene ontology analyses of potential CD24 interaction partners.

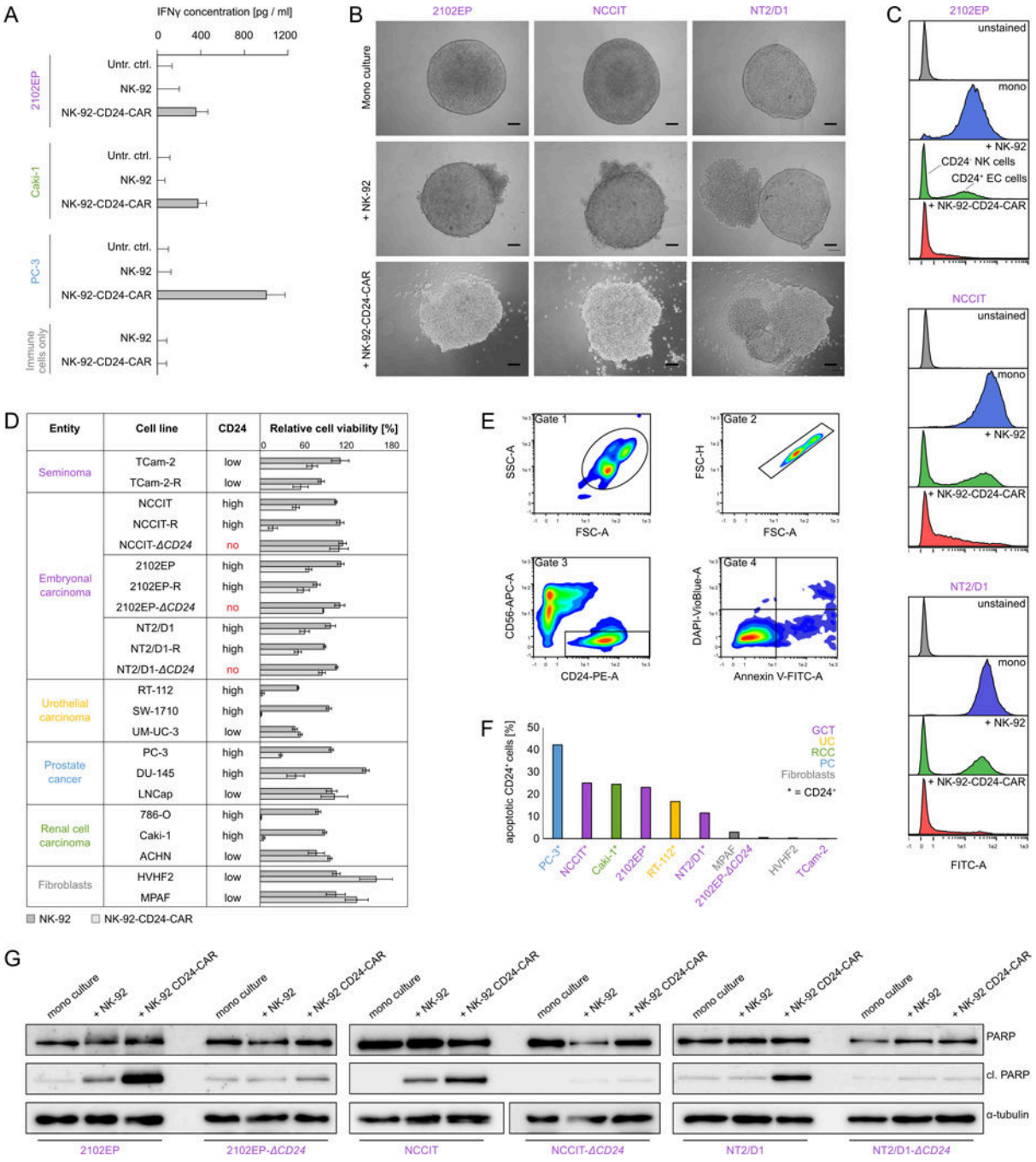

Figure 3:

A) ELISA assays indicating elevated IFNγ levels and, therefore, activation of NK-92-CD24-CAR cells upon co-culture with $CD24^+$ tumor cells in comparison with NK-92 cells or mono-cultures (n = 3). Error bars are indicated by means of SD. B) Macroscopic visualization of 3D cell aggregates of EC cells alone (2102EP, NCCIT, NT2/D1) or upon co-culture with NK-92-CD24-CAR cells after 24 h (right panel) (n = 25). Scale bar = 100 μm. C) Flow cytometric evaluation of CD24-FITC staining in dissociated 3D cell aggregates shown in B) compared to an unstained control (n = 25). D) Summarizing

bar graphs of relative cell viability of 20 tumor cell lines as well as fibroblast controls (HVHF2, MPAF) upon co-culture with NK-92 or NK-92-CD24-CAR cells (ratio 5 : 1) for 48 h (n = 4). Error bars are indicated by means of SD. E) Representative flow cytometric gating strategy to evaluate apoptosis induction (Annexin V / DAPI) in tumor cells ($CD24^+$) after 24 h of co-culture with NK-92-CD24-CAR cells ($CD56^+$). Cellular debris and doublets were excluded by using the side-scatter signals (SSC-width and SSC-height). F) Relative apoptosis induction in $CD24^+$ tumor cell lines (PC-3, NCCIT, Caki-1, 2102EP, RT-112, NT2/D1) as well as $CD24^-$ cells (2102EP-Δ*CD24*, TCam-2) and non-malignant fibroblasts (MPAF, HVHF2) upon co-culture with NK-92-CD24-CAR cells. Measurements were normalized against co-cultures with NK-92 cells. G) Western blot analyses of PARP cleavage and total PARP in EC cells (including Δ*CD24* sublines) co-cultured with either NK-92 or NK-92-CD24-CAR cells as compared to the untreated control. α-tubulin served as a loading control.

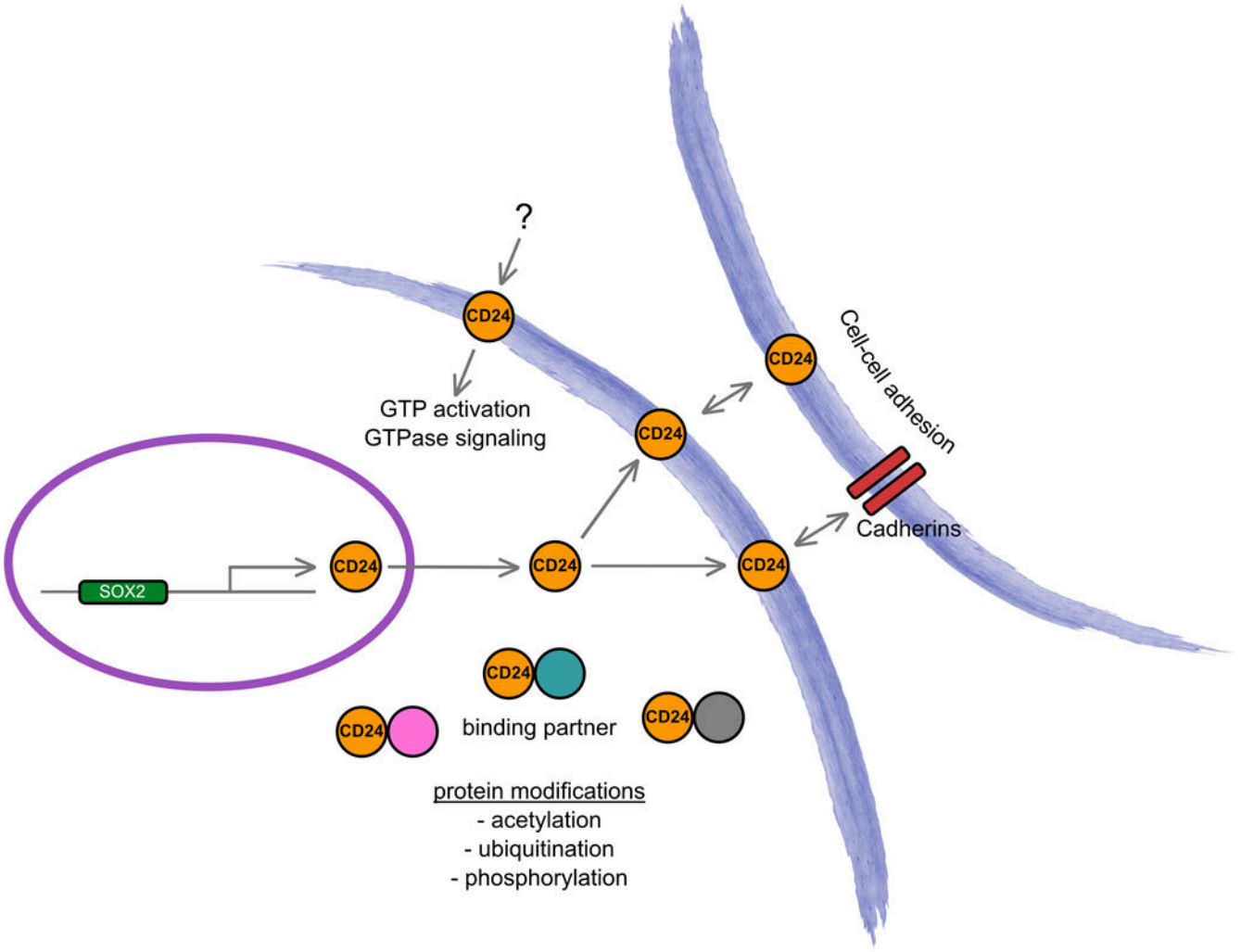

Figure 4:
Model summarizing the regulation and molecular function of CD24 in urological malignancies.